Impact of the assimilation of Atmospheric Infrared Sounder radiance measurements on short-term weather forecasts

Will McCarty,[1,2] Gary Jedlovec,[3] and Timothy L. Miller[3]

Received 14 December 2008; revised 22 April 2009; accepted 10 June 2009; published 29 September 2009.

[1] Advanced spaceborne instruments have the ability to improve the horizontal and vertical characterization of temperature and water vapor in the atmosphere through the explicit use of hyperspectral thermal infrared radiance measurements. The incorporation of these measurements into a data assimilation system provides a means to continuously characterize a three-dimensional, instantaneous atmospheric state necessary for the time integration of numerical weather forecasts. Measurements from the National Aeronautics and Space Administration (NASA) Atmospheric Infrared Sounder (AIRS) are incorporated into the grid point statistical interpolation (GSI) three-dimensional variational (3D-Var) assimilation system to provide improved initial conditions for use in a mesoscale modeling framework mimicking that of the operational North American Mesoscale (NAM) model. The methodologies for the incorporation of the measurements into the system are presented. Though the measurements have been shown to have a positive impact in global modeling systems, the measurements are further constrained in this system as the model top is physically lower than the global systems and there is no ozone characterization in the background state. For a study period, the measurements are shown to have positive impact on both the analysis state as well as subsequently spawned short-term (0–48 h) forecasts, particularly in forecasted geopotential height and precipitation fields. At 48 h, height anomaly correlations showed an improvement in forecast skill of 2.3 h relative to a system without the AIRS measurements. Similarly, the equitable threat and bias scores of precipitation forecasts of 25 mm $(6\ \mathrm{h})^{-1}$ were shown to be improved by 8% and 7%, respectively.

Citation: McCarty, W., G. Jedlovec, and T. L. Miller (2009), Impact of the assimilation of Atmospheric Infrared Sounder radiance measurements on short-term weather forecasts, *J. Geophys. Res.*, *114*, D18122, doi:10.1029/2008JD011626.

1. Introduction

[2] One of the primary limitations of numerical weather prediction relates to the accuracy and representativeness of the initial conditions of the atmosphere. Good forecasts require an accurate and spatially continuous characterization or analysis of the atmospheric state. This is problematic given the coarse and discontinuous observational networks in place around the globe. The concept of data assimilation is to interpolate these observations to a grid, typically by blending them with a guess of the atmospheric state to develop an optimal analysis to spawn a forecast. Owing to the nature of the various observation networks, many regions void of direct measurements of atmospheric quantities exist. While this problem is most significant in the Southern Hemisphere, it is still an issue in regions such as the Northern Hemispheric Pacific Ocean, the Northern Atlantic, the Caribbean Sea, and the Gulf of Mexico where direct measurements are still very limited.

[3] To compensate for the lack of direct measurements in the data void regions, many meteorological centers, including the National Centers for Environmental Prediction (NCEP), United Kingdom Meteorological Office (UKMO), Météo-France, and European Center for Medium-range Weather Forecast (ECMWF), routinely use the assimilation of satellite measured radiances into weather forecast models [e.g., *Derber and Wu*, 1998; *McNally et al.*, 2000; *Le Marshall et al.*, 2006; *McNally et al.*, 2006]. However, the use of radiances is not without complications, stemming from the sheer volume of the radiance data and the transformations necessary between radiance and analysis space. Furthermore, the presence of higher-order radiative processes associated with clouds and precipitation can further complicate the use of satellite radiance measurements within a data assimilation system.

[4] Under the Earth Observing System (EOS) initiative, NASA has launched a number of satellites to improve our understanding and prediction of the Earth system. Most notable to this study is the Atmospheric Infrared Sounder (AIRS) [*Aumann et al.*, 2003], which is a hyperspectral

[1]Global Modeling and Assimilation Office, NASA Goddard Space Flight Center, Goddard Earth Sciences and Technology Center, University of Maryland Baltimore County, Greenbelt, Maryland, USA.
[2]Formerly at Atmospheric Science Department, University of Alabama in Huntsville, Huntsville, Alabama, USA.
[3]Earth Science Office, NASA Marshall Space Flight Center, Huntsville, Alabama, USA.

Copyright 2009 by the American Geophysical Union.
0148-0227/09/2008JD011626

grating spectrometer measuring upwelling radiation from the Earth-atmosphere system in portions of the thermal infrared spectrum. Its greater spectral resolution produces 2 orders of magnitude more data than heritage instruments, thus improving the instrument's ability to vertically characterize the atmosphere. The applicability of AIRS within a data assimilation context is apparent, though problematic due to the large data volume (35 gigabytes of data per day) and operational weather forecasting constraints including the timeliness of the data delivery and assimilation execution. The AIRS data volume is often substantially reduced by "super-obing" instantaneous fields of view (IFOVs) spatially and using a spectrally thinned set of channels [*Goldberg et al.*, 2003; *Fourrié and Thépaut*, 2003]. Additionally, conservative cloud screening techniques often limit the radiances to predominately clear regions. Thus only a small portion of the data, as little as 1% on the global scale [*Chahine et al.*, 2006; *Goldberg et al.*, 2003], actually makes it to the assimilation process. The use of similar approaches within the constraints of regional models further limits the amount of spectral data available for assimilation to a fraction of a percent. This reduction in data usage is somewhat offset by the ability to use additional spatial data on the finer-scale regional model domain. Therefore it is very important to consider the differences between global and regional assimilation strategies for the proper utilization of AIRS radiance data. Differences in horizontal and vertical model grid spacing between a global and regional system result in different spatial thinning radii and methodologies for each scale. Similarly, different vertical characterizations within the models will result in different applicability of individual channels to a data assimilation system.

[5] AIRS measurements have the ability to improve the prediction of sensible weather elements within a regional forecast model and methodologies have been developed to fully maximize the use of the data, both in clear and cloudy footprints [e.g., *McNally and Watts*, 2003]. The study described in this paper presents methodologies used to assimilate AIRS measurements into a pseudo-operational framework emulating that of the North American Model (NAM) at NCEP. Proper spectral and spatial thinning methodologies were employed based on the strengths and limitations of the system. The impact of the measurements was assessed on the analysis step and short-term (0–48 h) forecasts spawned from the new analyses.

2. Background

[6] The AIRS instrument [*Aumann et al.*, 2003] on board the NASA EOS Aqua platform [*Parkinson*, 2003] is a hyperspectral infrared spectrometer that measures 2378 channels within a spectral range of 3.7 to 15.4 μm. The instrument has a 13.5 km spatial footprint at nadir, equating to a 1.1° IFOV, and a ± 49.5° (1650 km) scan width. AIRS Level-1B (L1B) calibrated radiances [*Pagano et al.*, 2003] are routinely available for near real time weather applications on a global basis. AIRS radiances are currently used operationally by NCEP in the Global Forecast System (GFS) model and the North American Model (NAM). *Le Marshall et al.* [2006] have shown that highly thinned cloud-free radiances provide improvements at all forecast times in 500 hPa height anomaly correlations for medium range forecasts in the GFS. The improvement of global modeling forecasts should trickle down to the improvement of regional modeling forecasts, as the measurements themselves are improving the initial analysis.

[7] Other studies have considered the assimilation of AIRS temperature and moisture profiles into weather forecast models [e.g., *Reale et al.*, 2008]. These studies used the vertical temperature, and in some cases the moisture, profile retrievals derived from cloud-cleared AIRS radiance data, which are provided by the AIRS science team [*Susskind et al.*, 2003]. Traditionally, the use of the retrieved products (versus the radiances) has not been optimal [*Errico et al.*, 2000], as inversion techniques used to retrieve atmospheric temperature and moisture information from satellite radiance measurements are known to smooth the vertical thermodynamic structure of the atmosphere because of the constraints and a priori conditions used in the retrieval process [*Susskind et al.*, 2003; *Rodgers*, 1990], thus adding retrieval error to the preexisting observation uncertainty. Broad weighting functions and spatial averaging (50 km spatial resolution for the current profiles produced by the AIRS science team) also contribute to the loss of small-scale information. The accuracy of retrievals of temperature and moisture profiles from AIRS has dramatically improved over heritage measurements, however, with an accuracy of 1 K in 1 km layers and 15% humidity in 2 km layers for temperature and moisture, respectively when compared to radiosondes [*Divakarla et al.*, 2006; *Tobin et al.*, 2006].

[8] Over the years, operational weather forecasting has shifted away from the use of profiles in data assimilation. The retrieved temperature and moisture profiles from filter radiometers did not provide the accuracy and vertical resolution required of forecast models, having a generally negative impact in the data-rich Northern Hemisphere [*Andersson et al.*, 1991]. The impact of heritage radiances measurements from the TIROS Operational Vertical Sounder (TOVS) data sets on global systems has shown significant improvements, doubling the forecast accuracy at 5 days versus the assimilation of profiles [*Derber and Wu*, 1998]. While the largest impact in the global systems has been seen in the Southern Hemisphere, the addition of radiances to the operational systems has shown positive impacts globally, even in the relatively data-rich Northern Hemisphere midlatitudes [*McNally et al.*, 2000; *English et al.*, 2000]. The direct assimilation of AIRS radiances in the analysis process circumvents many of the procedures that reduce the information content and utility of the temperature and moisture profiles.

[9] The assimilation of direct radiance observations is complicated by the nonlinear relationship between the analysis and radiance space. The implementation of variational assimilation systems has allowed for the ability to assimilate radiance measurements by eliminating the linearity requirement necessary in heritage approaches [*Derber and Wu*, 1998]. The conversion of the analysis state to observation space requires the use of a forward operator. In radiances, the accuracy of the forward radiative transfer needs to be balanced with the speed in which the forward calculations are performed. Fast radiative transfer algorithms have been created [e.g., *Han et al.*, 2006; *Strow et al.*, 2003], maintaining accuracy that exceeds instrument noise while reducing the computational expense by utilizing parameterizations of the absorption lines of the atmosphere to generate the

Table 1. Data Assimilated in the Study for the CNTL Experiment Separated by Ground-Based and Space-Based Observations[a]

Observation	Platform
Ground-Based	
Upper air	sonde
	aircraft
Land surface	SYNOP
	METAR
Marine surface	buoy
	ships
Radial winds	**WSR-88D**
Radar vertical winds	**Wind profiler**
Precipitable water	**SuomiNet/GPS**
Satellite-Based	
Satellite winds	**GOES**
	MODIS Polar
	SSM/I
Precipitable water	**SSM/I**
Infrared radiances	**GOES sounder**
	HIRS
Microwave radiances	**AMSU-A**
	AMSU-B
	MHS

[a]Bold indicates measurements that are remotely sensed.

necessary atmospheric transmittances to simulate observations from the analysis state.

3. Assimilation and Modeling System

[10] In this study, the grid point statistical interpolation (GSI) [*Wu et al.*, 2002] analysis system is used for the generation of the initial state conditions. It is a three-dimensional variational (3D-Var) assimilation [*Lorenc*, 1981] scheme cooperatively developed and utilized by NCEP, the NASA Global Modeling and Assimilation Office (GMAO), the Global Systems Division (GSD) of the Earth System Research Laboratory (ESRL), and the JCSDA. It is capable of assimilating data from many different observational platforms including radiance measurements obtained from satellites. The GSI is designed for both global and regional scale applications and provides initial conditions for the Weather Research and Forecast (WRF) modeling systems [*Michalakes et al.*, 2004].

[11] For the assimilation of satellite radiances, it is necessary to be able to convert the background state vector to radiance space for the calculation of the observation residuals. For this, the Community Radiative Transfer Model (CRTM) [*Han et al.*, 2006] has been linked to the GSI. The CRTM is an advanced forward radiative transfer package that balances the need for speed and accuracy in simulating satellite radiance measurements in all portions of the electromagnetic spectrum from a given atmospheric state. For this application, the most notable and necessary portion of its advanced physics is the rapid gas absorption model, which is capable of quickly generating the necessary absorption coefficients, and thus forward, tangent linear, and adjoint calculations, necessary for the assimilation of radiances.

[12] A previous forecast valid at analysis time has been used to define the background state vector. Forecasts in this study have been integrated using the Nonhydrostatic Mesoscale Model dynamic core of the WRF framework (WRF-NMM) [*Janjic et al.*, 2001]. The models that utilize the WRF framework are intended for a wide range of applications, from idealized research to operational forecasting and are flexible, portable, and state-of-the-art atmospheric simulation systems. On the basis of their merits, models utilizing its framework are replacing existing forecast models, such as the MM5, the RUC system at NOAA/ESRL/GSD, and the Eta model at NOAA/NCEP. The WRF-NMM is the current North American Model (NAM) at NCEP and is fully compatible with the GSI. As a result of improved horizontal grid spacing, the NMM dynamic core treats the nonhydrostatic processes by considering a mass-based σ coordinate and by separating atmospheric flows into hydrostatic and nonhydrostatic processes. It is noted that model space differs from analysis space. Thus a transformation is necessary to convert the background state vector to analysis space.

4. Assimilated Data

4.1. Commonly Assimilated Data

[13] The data assimilated in this study was that of the operational National Data Assimilation System (NDAS) during the period of study, with the only exception being that only the Level II and Level III (NIDS) WSR-88D radial wind superobservations were used instead of the full resolution measurements. These data are listed in Table 1 and include observations from both ground-based and spaceborne platforms. While the two platform categories have a similar number of observation types, the vast majority of the data volume comes from satellite sources, with radiance data sets dominating. These are the data sets that make up the control for this study.

4.2. Experimental Data

[14] In addition to the aforementioned data, the use of AIRS data within the assimilation system was the experimental variable. AIRS Level-1B (L1B) calibrated radiances [*Pagano et al.*, 2003] are routinely available for analysis and in near real time weather applications on a global basis. A 281 channel subset [*Goldberg et al.*, 2003] is available to operational centers at every footprint for assimilation purposes, as denoted in Figure 1. The subset consists of channels from the 15 μm CO_2, 9.6 μm O_3, 6.7 μm H_2O_v, and 4 μm CO_2 absorption continua, as well as the 11 μm atmospheric window. The channel subset was selected prelaunch based on four criteria; the channels must (1) correspond with wings of absorption lines, (2) be sensitive to one primary absorbing constituent, (3) have a near-constant surface emissivity, and (4) utilize the short wavelengths (C. Barnet, personal communication, 2005). Within the analysis system, surface characteristics, such as land classification type, corresponding to the observations are determined from inputted masks. The representativeness errors associated with the observations are partially a function of surface type. Water surfaces have the least error, due to the corresponding surface emissivity being more predictable than land, ice, and snow surfaces. Channel rejection based on the detection of clouds is also performed using a technique that is common to the entire thermal infrared spectrum and is both channel and instrument independent, which allows channels unaffected by clouds within a cloudy footprint to be considered in the assimilation process (J. Derber, personal communication, 2009).

5. AIRS Channel Selection and Assimilation

[15] Not all of the 281 channels available for assimilation are applicable in the presented framework because they

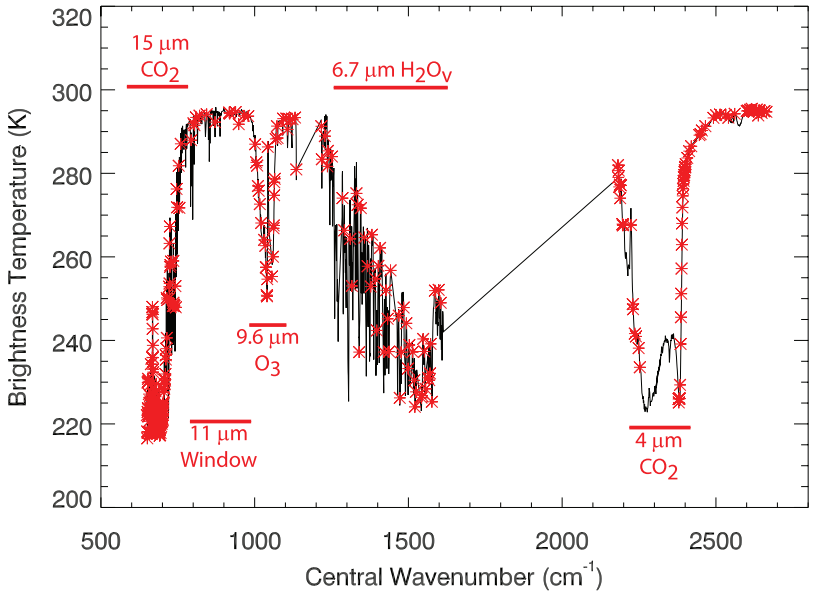

Figure 1. An example AIRS spectrum (black) and the corresponding 281 channels (red stars) that are delivered to NCEP for operations. Red lines and text denote notable absorption continua within the spectrum.

cannot be properly represented within the model or analysis space. This determination was based on the following sensitivity analysis. For a midlatitude summer profile, the brightness temperature sensitivity, δT_b^j, for channel j of the 281 channel subset, defined as

$$\delta T_b^j = \frac{\partial T_b^j}{\partial q^i}(\delta q^i), \tag{1}$$

was investigated, where q^i is one of the three state variables used in forward calculations, expressly temperature, specific humidity, or volumetric ozone mixing ratio at a given vertical level i. A finite perturbation, represented by δq^i, in the specified quantity (1% for temperature and 10% for specific humidity and ozone) was applied to the Jacobian, $\partial T_b^j/\partial q^i$, or change in a channel's calculated brightness temperature with respect to the state variable. The purpose of considering this defined sensitivity, and not the Jacobian itself, was because the Jacobian can misrepresent the true sensitivity of the brightness temperature to a reasonable change in the atmospheric quantity [*Chevallier and Mahfouf*, 2001]. Specific humidity, for example, can vary by 3 orders of magnitude between the top and bottom of the troposphere. Additionally, the perturbation percentages were chosen so that the brightness temperature sensitivities were of the same order of magnitude. The sensitivity of each channel to realistic perturbations of the atmospheric state was used to select the channels applicable to the assimilation system in this study and is shown in Figure 2.

[16] The use of AIRS data within the framework of this study is limited by four primary factors. First, of the 281 channel subset, those which had significant atmospheric contribution from above the model top, 2 hPa, to the top of the radiative transfer model, 0.01 hPa, were inappropriate for use in this assimilation system and were discarded. For this analysis, the total contribution above the top of the model is determined as

$$\Delta T_b^{>TOA} = \sum_{i=2hPa}^{0.01hPa} \delta T_b^i, \tag{2}$$

where channels with $\Delta T_b^{>TOA}$ larger than 0.06 K were discarded. This is equivalent to roughly 25% of the noise-equivalent delta temperature of the least noisy channels for the spectral region of most concern, the 15 μm CO_2 absorption continuum, as apparent in Figure 2. This threshold is explicitly conservative, as this analysis is limited by the use of only a single climatological profile, though multiple climatological profiles were investigated (not shown), and no scan angle dependency is considered to avoid the necessary consideration of scan angle bias within the CRTM. Second, any channels with significant ozone absorption (Figure 2c) are discarded, as ozone is not a model variable in this study. Therefore no accurate background estimate existed in the analysis state. While a few channels within the 15 μm CO_2 absorption continuum were discarded by this criterion, the bulk of eliminated channels by this criterion are in the 9.6 μm O_3 absorption continuum. Third, no shortwave (<5 μm) channels were used in the assimilation process. Relative to the 15 μm CO_2 absorption continuum, they are generally less sensitive to absorption by constituents other than CO_2 and have sharper weighting functions in the lower troposphere [*Susskind and Kouvaris*, 2006]. They are also, however, sensitive to reflected solar radiation. The consideration of this reflected component in the assimilation system would be an additional variable that would require the performance of the instrument to be considered separately in both local day and night situations. Finally, channels that have specific onboard performance issues were eliminated as their high noise or unpredictable behavior result in them unreliable for assim-

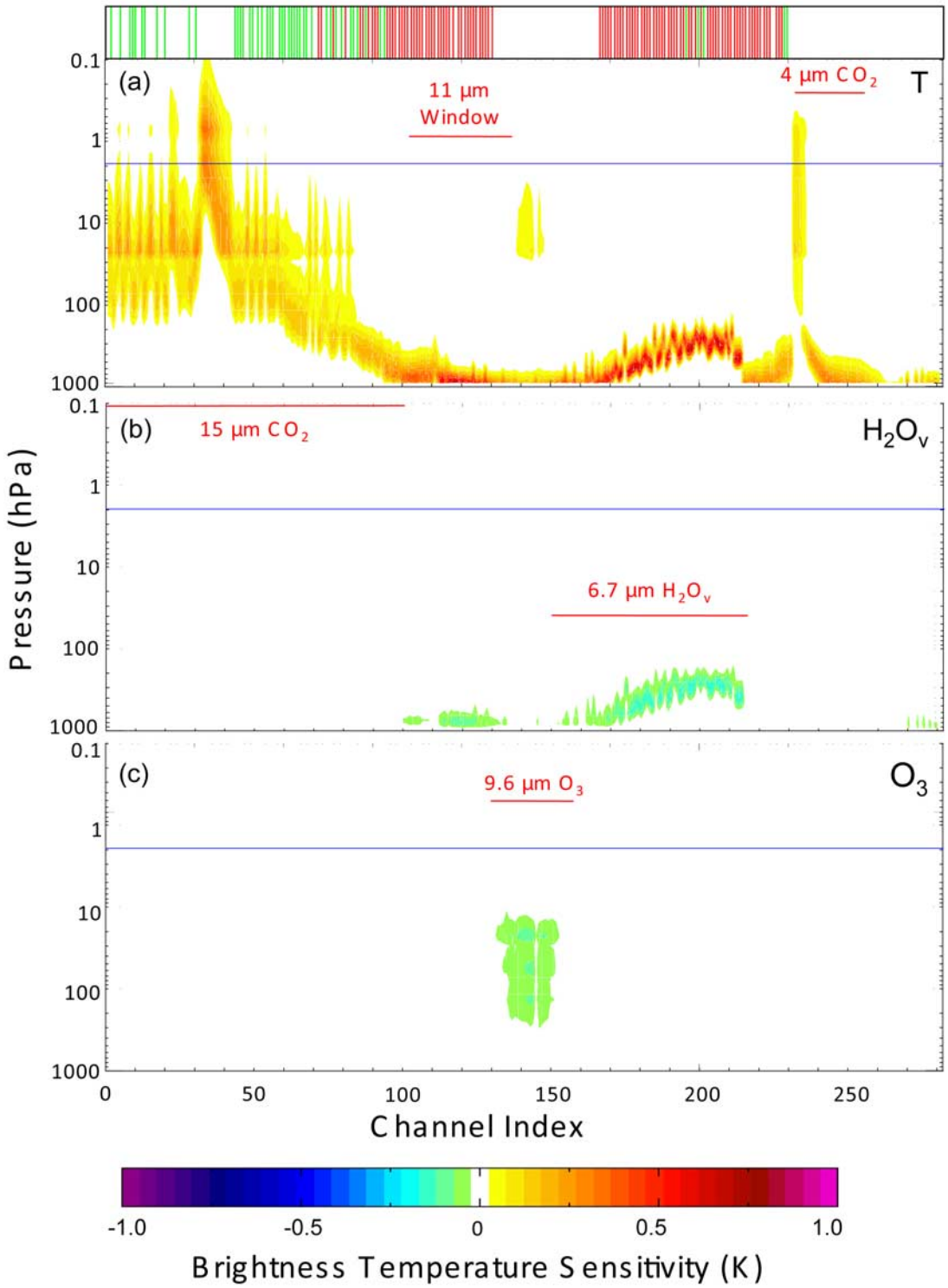

Figure 2. The brightness temperature sensitivities, as a function of model state variables (a) temperature, (b) specific humidity, and (c) volumetric ozone mixing ratio valid at each pressure. Also denoted are the primary absorption continua over the 281 AIRS channels (red) and the model top (blue). The tick marks above the graphs indicate channels selected for use in the AIRS experiment (red) and the GDAS (green, red inclusive).

ilation, based on AIRS channel properties and quality control flags distributed by the AIRS Science Team.

[17] In the operational Global Data Assimilation System (GDAS), 151 of the 281 AIRS channels [*Le Marshall et al.*, 2006] have previously been selected for use. Owing to the aforementioned constraints, however, the experimental system described in this study used 103 channels selected for assimilation (Figure 2). Though not a criterion for channel

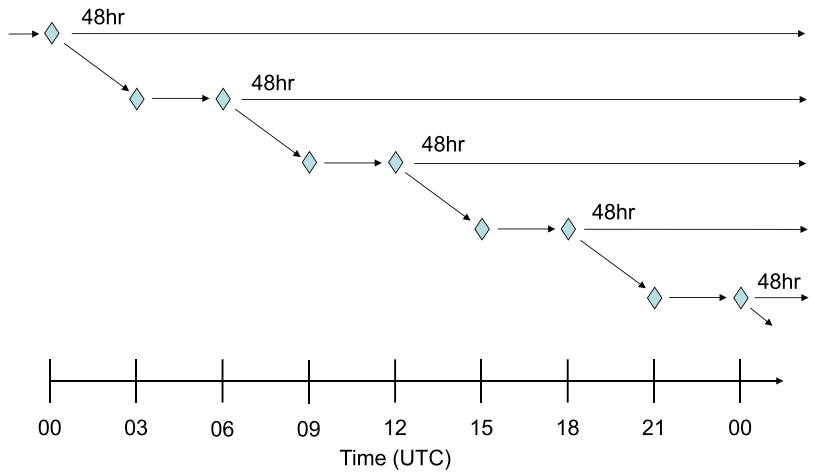

Figure 3. The assimilation cycle for the AIRS and CNTL runs. Arrows indicate model iterations run to either generate the background field for assimilation (diamonds) or for spawned forecasts for weather prediction purpose (denoted by 48 h).

selection, all of the 103 channels selected for regional assimilation are contained in the 151 channels used in the GDAS, likely due to similar selection criteria.

[18] Horizontal thinning is also performed on AIRS measurements within the analysis system. While every footprint is available, corresponding to a 13.5 km spatial resolution at nadir, a 60 km sampling mesh was selected to thin the data for assimilation, which is consistent with heritage thermal infrared instruments and corresponds to $5\Delta x$ on the 12 km grid. The use of every footprint could result in the introduction of spurious gravity waves into the model, as adjustments would be near the level of grid spacing and result in poor resolution of features leading to computational instability [*Pielke*, 1991], though the adjustments would be largely smoothed by the distribution of information via the background error covariance matrix. The thinning mesh differs from the global system, which uses a 180 km sampling. As a result of less spatial thinning, this experiment considered a factor of nine more AIRS footprints in areas common to the NDAS and GDAS for assimilation.

6. Assimilation Cycle and Timeframe

[19] Two runs were performed in this research, with the control being all of the aforementioned commonly assimilated data (CNTL hereinafter, Table 1) and the experiment being all commonly assimilated data with the addition of AIRS radiances (AIRS hereinafter). Thus differences presented only correspond to the addition of AIRS data to the data assimilation system.

[20] The assimilation cycle used in this research is presented in Figure 3. The window for observations was ±1.5 h, with assimilation performed every 3 h. The background state vector, a 3 h WRF-NMM forecast valid at analysis time, is represented by the arrows between assimilation steps. The assimilation cycle presented is continuous in that the cycle repeated daily at 0000 UTC, using a 3 h forecast initialized at 2100 UTC the previous day as the background. Forecasts were spawned from the analyses four times a day at 0000, 0600, 1200, and 1800 UTC and were run to 48 h past model initialization, as denoted by arrows extending horizontally from the analysis state. The model domain corresponds to the full NAM 12 km (NAM12) grid, equivalent to the operational grid at NCEP. Since the purpose of the operational model is for forecasts over continental North America, the large domain allows for information from boundary conditions to be adjusted by the assimilation process before propagating over the CONUS. The background error covariance matrix was that of the operational system, developed using the methodologies presented by *Wu* [2005].

[21] The study was performed on analyses and forecasts spawned over a week long period starting at 0000 UTC on 9 April 2007 through 0000 UTC on 16 April 2007. Prior to this period, however, from 26 March 2007 through 8 April 2007, the assimilation cycle was performed for both the AIRS and CNTL experiments separately for two primary reasons. First, it allowed the additional AIRS data within the analysis to propagate through the background. If the addition of the AIRS measurements is resulting in a more accurate analysis state, the 3-h forecasts between assimilation steps will potentially be improved. Thus the background state of the analysis is improved. The background state vectors for the AIRS experiment are thus inherently different than those of the CNTL. Second, for the AIRS experiment, it allowed the satellite bias corrections within the GSI system [*Derber and Wu*, 1998] to stabilize, since their initial values were set to zero. By doing this 2 weeks prior to this study, the bias correction coefficients stabilized early in the cycle, and any negative impact imposed on the analysis state by the bias corrections prior to stabilization had propagated out of the domain before the week of analyses and forecasts of focus.

[22] Meteorologically, the period of the 9–16 April 2007 was active. The mean 500 hPa height anomalies over the validation period, which extends to 0000 UTC 18 April 2007 because the final forecasts are spawned to 48 h on 16 April 2007, are presented in Figure 4. The negative mean anomaly regions reflect the preferred storm track over the period, as indicative of the major storm tracks determined by tracing the negative 500 hPa height anomaly minima through time over the validation period. Over the continental United States, two cyclogenesis events, with one originating over eastern Colorado and the other being a nor'easter, dominate

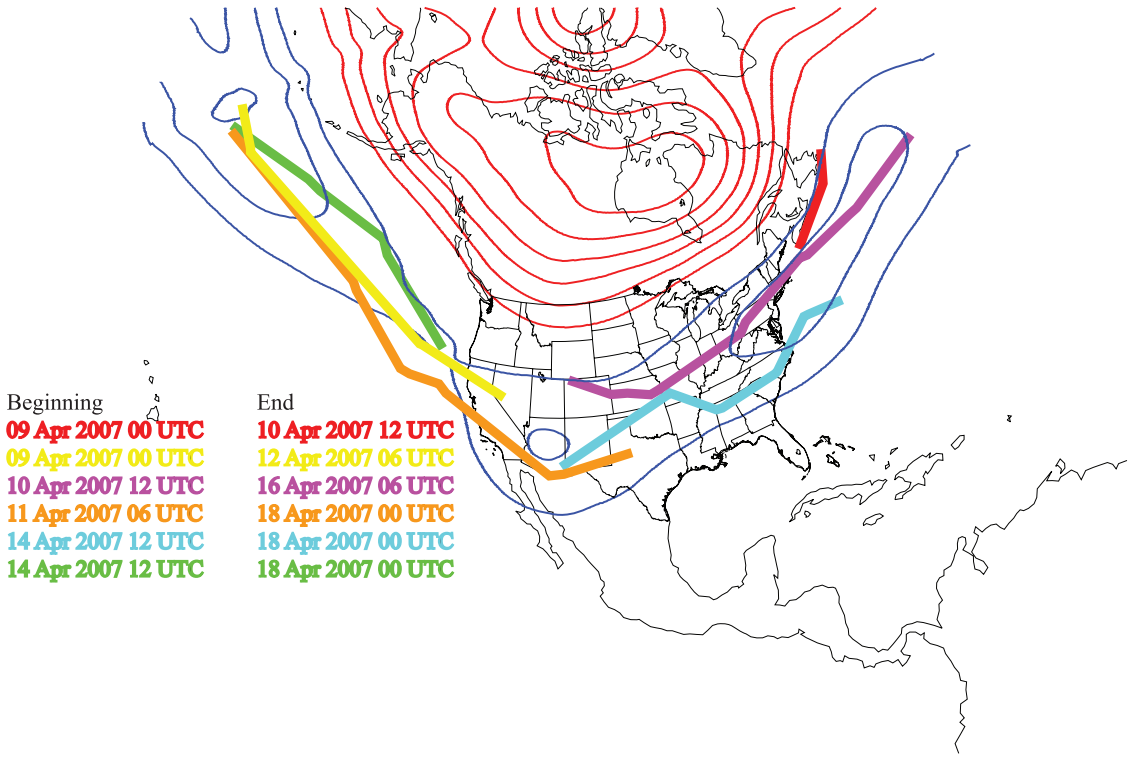

Figure 4. Mean 500 hPa height anomalies for 0000 UTC 9 April 2007 through 0000 UTC 18 April 2007, contoured every 60 m for positive (red) and negative (blue) anomalies. The thick lines correspond to storm tracks, determined by tracking 500 hPa height anomaly minima through the period, and correspond, by color, to the time periods listed.

the signal over the 2-week period. Both events developed into strong midlatitude cyclones associated with strong baroclinicity and deep central seal-level pressure, with minima of 991 and 982 hPa, respectively, during the analysis period. The variability in the atmospheric structure over the period allowed for the impact of AIRS measurements on high impact weather events to be investigated in this study.

7. Results

[23] The effects of using AIRS measurements in the data assimilation system and subsequent forecasts are described in the following sections. The changes imposed by the addition of AIRS data are demonstrated by evaluating the differences in the analysis fields relative to the CNTL. After the impact assessment, the changes were then validated over the study period, assessing the improvement of the analyses directly versus independent measurements. Since few independent measurements coincided to the analyses, the verification of short-term forecasts over the study period is presented to assess the impact of the AIRS data.

7.1. Analysis Impact

[24] It is desirable to evaluate the effect of assimilating the AIRS radiances on the analysis before the forecast cycle begins by differencing the experimental and control analyses. This investigation showed the combined effects of the direct assimilation and the propagated, or indirect, impact from earlier assimilations through the background fields. An example of this is shown with the 500 hPa geopotential height difference fields in Figure 5 for the four daily analysis times on 9 April 2007. The 500 hPa height fields are clearly changed by the inclusion of AIRS data. Most changes occur over the oceans where AIRS data is routinely assimilated over the spin up period. While these changes are small, typically <10 m, they are consistently adjusted in each forecast cycle. The swath width of the AIRS data for the current assimilation times (green) indicates the typical region of coverage for the AIRS scans. Recall that the assimilation cycle only includes AIRS data within ±1.5 h of the assimilation time limiting the regions where AIRS data is assimilated. The difference fields are larger over these swath regions indicating a greater effect from the direct assimilation of AIRS data (at the analysis times) versus the indirect impact, though both impacts are evident. As a result of the orbital characteristics of AIRS, the figure indicates larger direct impacts over the Pacific at 0000 and 1200 UTC assimilations versus the Gulf of Mexico and Atlantic, while the opposite held true over the 0600 and 1800 UTC assimilations.

[25] The largest impact areas are seen over oceanic portions of the domain and in regions which were poorly sampled by more conventional measurements, such as northern Canada and the southeastern portion of the NAM12 domain. The impact over land is less apparent because the accumulated effect of the relative weighting of AIRS versus other conventional observations prevalent over land, the increased uncertainty in the lower tropospheric sensing channels over land due to surface emissivity characterizations, and the higher accuracy of background state versus

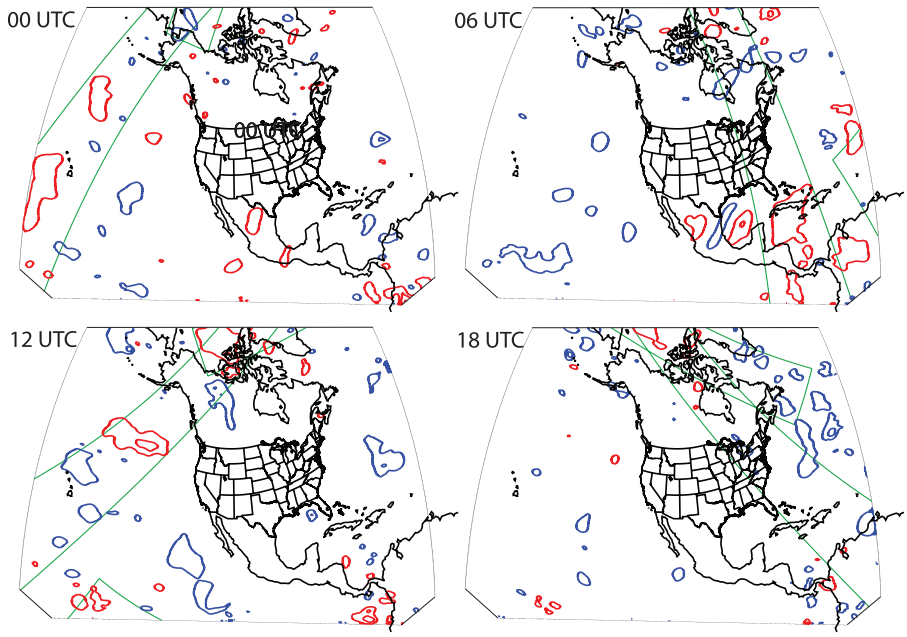

Figure 5. The difference between the analyzed 500 hPa geopotential height fields of the AIRS and CNTL assimilation cycles on 9 April 2007. The contours are every 5 m, with blue (red) contours indicating negative (positive) differences. The AIRS overpasses applicable at time of assimilation are outlined in green. All four analyses corresponding to the full forecast integration times are shown.

oceanic regions. The decreased uncertainty in the background field is because the CONUS is both well observed and generally downstream of data rich regions.

7.2. Analysis Validation

[26] The direct validation of the analysis state is inherently problematic because of the lack of independent observations. Since the study emulated an operational system, it utilized conventional observations to develop the most robust analysis possible. Most low error validation data and conventional measurements, such as temperature and moisture from surface observation sites and radiosondes, were assimilated into the analysis and thus not independent. One of the few data sources not used in the assimilation process was the GOES-11 Sounder [*Menzel and Purdom*, 1994], a multispectral scanner with 18 thermal infrared channels from 14.7 to 3.76 μm which at this time was operating as the western GOES satellite positioned over the equator at 135°W longitude. This data had not yet been assimilated operationally in the NDAS. The measurements from this platform were used as an independent validation data set over the Pacific Ocean, corresponding to a region where AIRS observations were shown to make notable changes to the analysis (Figure 5).

[27] Comparison of the analysis state to the GOES Sounder observations requires a transformation of either the analysis to observation space or the observations to analysis space. The former is performed, generating calculated GOES Sounder brightness temperatures via the CRTM for comparison to the observed brightness temperatures for the same channels. This approach was used because forward calculations via the CRTM are more accurate than the inversion of the observations to profile space. The profiles derived from the GOES Sounder channels are insufficient for direct comparison to model data in analysis space because of their lack of information on the vertical structure of the atmosphere resulting from only a few independent pieces of information in the 18 Sounder channels.

[28] A comparison of calculated (from analysis fields) and observed GOES-11 Sounder channel brightness temperatures was made for the 29 analyses (four per day for 7 days plus one analysis period) using cloud-free and coincident points over the study region. The correlation between the observed and calculated brightness temperatures for both the CNTL and AIRS experiments is presented in Figure 6. The combined correlation results of all four forecast initialization times as a function of GOES Sounder channel are shown in Figure 6a. Channels 1, 2, and 12 comparisons depict notable differences between the control and AIRS experiments. The largest difference between the two experiments is in channel 2, which is primarily sensitive to emission from upper tropospheric carbon dioxide. By assuming CO_2 is well-mixed and constant in mass, the measured brightness temperatures correspond to the temperature in this layer. The improvement in channel 1 corresponds to better characterization of the layer-averaged temperature of the lower and middle stratosphere, while the slight improvement in channel 12 is due to the improved representation of upper tropospheric water vapor or temperature (or both). Thus the assimilated AIRS radiance data improves the model thermal structure consistent with the GOES observations.

[29] The difference in correlation between the control and AIRS experiments was separated by analysis time to better diagnose differences between the control and the analysis influenced by the AIRS data, as shown in Figure 6b. The 0000 UTC and 1200 UTC analyses show greater improvement than the 0600 UTC and 1800 UTC. In the 0600 UTC and 1800 UTC cycles, the AIRS observations assimilated in into the analysis occur over the eastern portion of the domain and thus had no direct effect on the portion of the analysis coincident to the GOES-11 Sounder measurements.

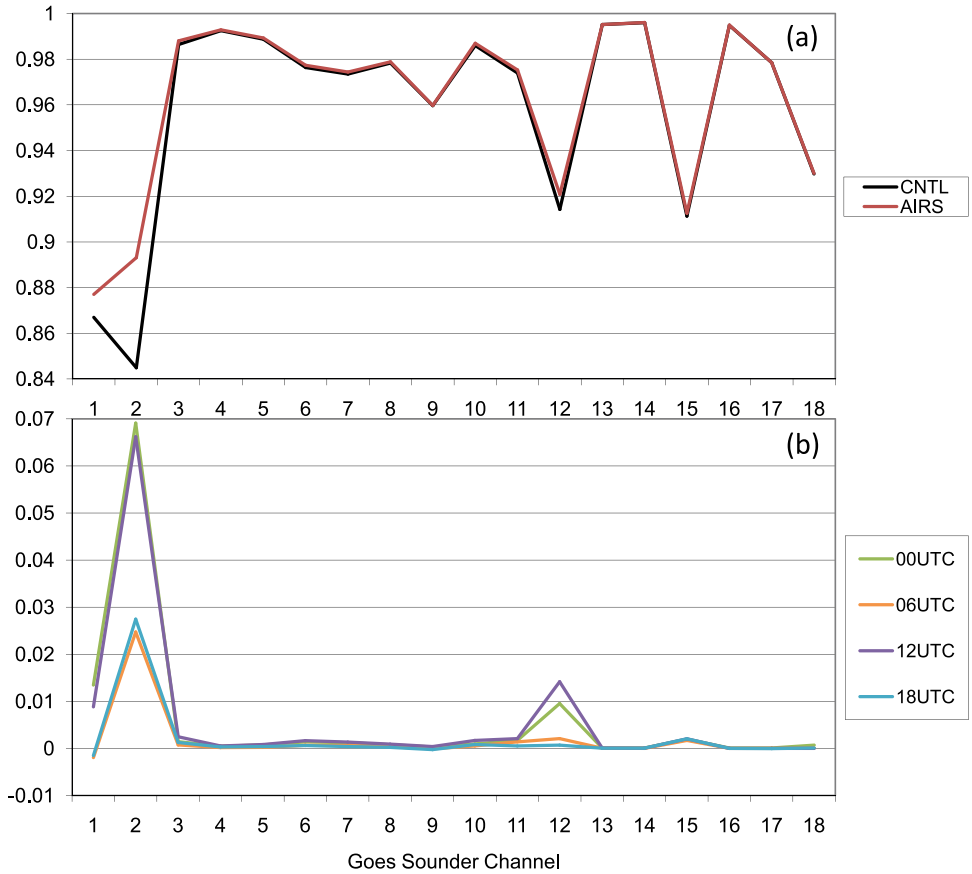

Figure 6. GOES-11 sounder brightness temperature (a) correlations for AIRS (red) and CNTL (black) for all cycles and (b) correlation differences (AIRS minus CNTL) separated for analyses at 0000 (green), 0600 (orange), 1200 (purple), and 1800 (blue) UTC cycles.

Improvements shown at these times are due to the propagated impact from the earlier cycles. For the 0000 UTC and 1200 UTC cycles, assimilated AIRS measurements spatially coincide with the GOES-11 observations, so the improvements are both direct from the assimilation process as well as indirect from the improvement in the background state.

7.3. Forecast Verification

[30] In order to investigate the impact of the improved analyses on the subsequent weather events, forecasts were spawned four times a day and run for 48 h past model initialization for each day from 0000 UTC on 9 April 2007 through 0000 UTC 16 April 2007 for a total of twenty-nine 48 h forecasts. A comparison of the forecasted atmospheric states to temporally corresponding analysis fields provides an assessment of the impact of the AIRS assimilated fields on the short-term weather forecasts. For all of the forecasts spawned over the 9–16 April 2007 timeframe, the height anomaly correlations were used as a standard measure for comparison [e.g., *Derber and Wu*, 1998; *McNally et al.*, 2000; *Le Marshall et al.*, 2006]. For this study, the anomalies were calculated as a function of latitudinal mean height, defined as

$$Z' = Z - \overline{Z}(\phi), \tag{3}$$

which eliminated the natural poleward decrease in height but did not remove the climatological mean. The correlations were calculated over the continental United States, with the two sample sets being the forecasted height anomaly at a given level and the corresponding CNTL analysis in time and space. The purpose of validating over the CONUS, versus the entire domain, is that the CONUS is well observed with conventional observations and the analysis field is therefore a close spatial representation of the truthful state of the atmosphere. Over the oceanic portion of the domain, there are far less conventional observations, and the accuracy of the verifying CNTL analysis is questionable and difficult to assess.

[31] The height anomaly correlations as a function of forecast hour at 500 hPa and 1000 hPa for both the control and AIRS experiment for all forecasts spawned during the 1-week period are presented in Figure 7. The AIRS experiment shows a consistent improvement in skill over the CNTL as the forecast progresses at both 500 hPa and 1000 hPa. At 48 h, a forecast improvement, defined as the time difference in hours of two points of equivalent anomaly correlation coefficient, is 2.3 h at 500 hPa, illustrating that the AIRS forecast at 48 h has the same skill as a CNTL forecast 2.3 h prior. It is noted that this estimate is obtained by an interpolation, since the height anomaly correlation calculations were performed every 6 h. Positive impact is also seen at

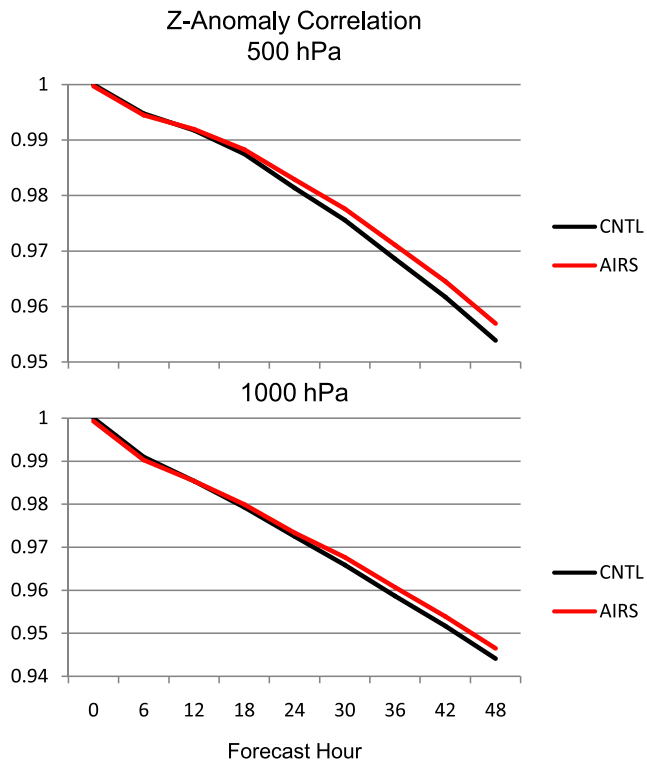

Figure 7. The (top) 500 hPa and (bottom) 1000 hPa height anomaly correlation for the AIRS (red) and CNTL (black) experiments.

1000 hPa with a forecast improvement of 1.9 h. Similar improvements were noted at other tropospheric levels (not shown). These increased correlations show that the forecasted atmospheric patterns, corresponding to the height anomalies, were more accurately forecasted over the study period with the inclusion of AIRS measurements in the data assimilation.

[32] The results above evaluated the anomaly correlations over the CONUS as a whole. The spatial variability of the impact of the AIRS measurements on 500 hPa geopotential heights is evaluated by calculating the root mean squared error (RMSE) for each grid point over all n forecasts initialized during the period of study for each experiment. Figure 8 shows the spatial distribution of the difference in mean squared error (ΔRMSE), as defined as

$$\Delta RMSE_{i,j}^{h} = \sqrt{\frac{1}{n}\left(\sum_{n}\left(Z_{Fcst}^{CNTL} - Z_{Anl}^{CNTL}\right)^{2}\right)_{i,j}^{h}} - \sqrt{\frac{1}{n}\left(\sum_{n}\left(Z_{Fcst}^{AIRS} - Z_{Anl}^{CNTL}\right)^{2}\right)_{i,j}^{h}} \quad (4)$$

at forecast hour h, where Z indicates geopotential height for the CNTL and AIRS experiments, and the forecasts, denoted by the *Fcst* subscript, were compared to corresponding analyses, denoted by the *Anl* subscript. The root mean squared error difference was used to quantify the absolute departure from the "truth," or corresponding analyses. Positive (negative) values of ΔRMSE indicate a net improvement (degradation) with the additional AIRS measurements in the assimilation cycle, or a reduction (increase) in RMSE. As expected, the absolute magnitude of ΔRMSE increases with forecast time. In the earlier hours, the magnitude of the ΔRMSE is relatively small. This is expected as the impact of the AIRS observations shown in Figure 5 was generally small, and the differences in the analyses were low enough to produce similar results at early forecast times. The AIRS 6 h results show little impact on forecasted height fields. Small regions of negative impact appear over data void regions where the information content is primarily carried through from the background field, which is, by nature, closer to the CNTL than the AIRS because the CNTL analyses are used for verification. At later forecast times the impact is largely positive, particularly over the data rich CONUS region. The largest positive impact area seems to originate over Colorado at 12 h and is observed over the central United States at 48 h. This maximum corresponds to the beginning of two storm tracks during the study period (Figure 4). The addition of AIRS data is having a positive impact on these cyclogenesis events, bringing the forecasted development of the events closer to the corresponding verification analyses.

[33] The largest negative impact is seen over the northwestern CONUS, though the magnitude of this negative impact is roughly 50% of that of the aforementioned positive impact maximum. The negative impact area seemed to propagate from the Gulf of Alaska southward with increasing forecast time. This oceanic area is sparsely observed, so the accuracy of verifying analyses is questionable because of a potential reliance on the background field, particularly at earlier forecast hours when the minimum is centered over the ocean. The fact that the minimum still exists as it propagated over land in the latter forecast times, where the corresponding analyses are more accurate due to increased observations, affirms that it was a real reduction in accuracy due to the addition of AIRS measurements to the analysis. This minimum may result from potentially cloud contaminated radiances entering the assimilation process and not being detected in the cloud screening inherent in the GSI system. To evaluate this occurrence, the Level-3 MODIS-derived weekly cloud analysis valid from 7 to 15 April 2007 was considered. The mean cloud fraction, presented in Figure 9, shows that the region was consistently cloudy, with >75% fractional cloudiness over the region over the vast majority of the Alaskan Gulf. Cloud top pressure fields (not shown) indicated that low clouds, ranging from 900 to 600 hPa, persisted over the region. Since AIRS is an infrared instrument and the polar regions do not have the vertical thermal contrast of that of the midlatitude and equatorial regions, detection of low clouds in the atmosphere is often troublesome due to climatologically persistent temperature inversions [*Wielicki and Coakley*, 1981] and the lack of cloud signal versus atmospheric emission and instrument noise in the 15 μm CO_2 absorption continuum [*Menzel et al.*, 2008]. Thus cloud contaminated measurements within this region were potentially assimilated and resulted in the degradation of the forecasts denoted by the propagation of error from this region as shown previously.

[34] The impact of AIRS measurements on the system as due to both direct AIRS measurements and the propagated impact through the background fields was previously discussed. Considering the MODIS cloud analysis upstream of

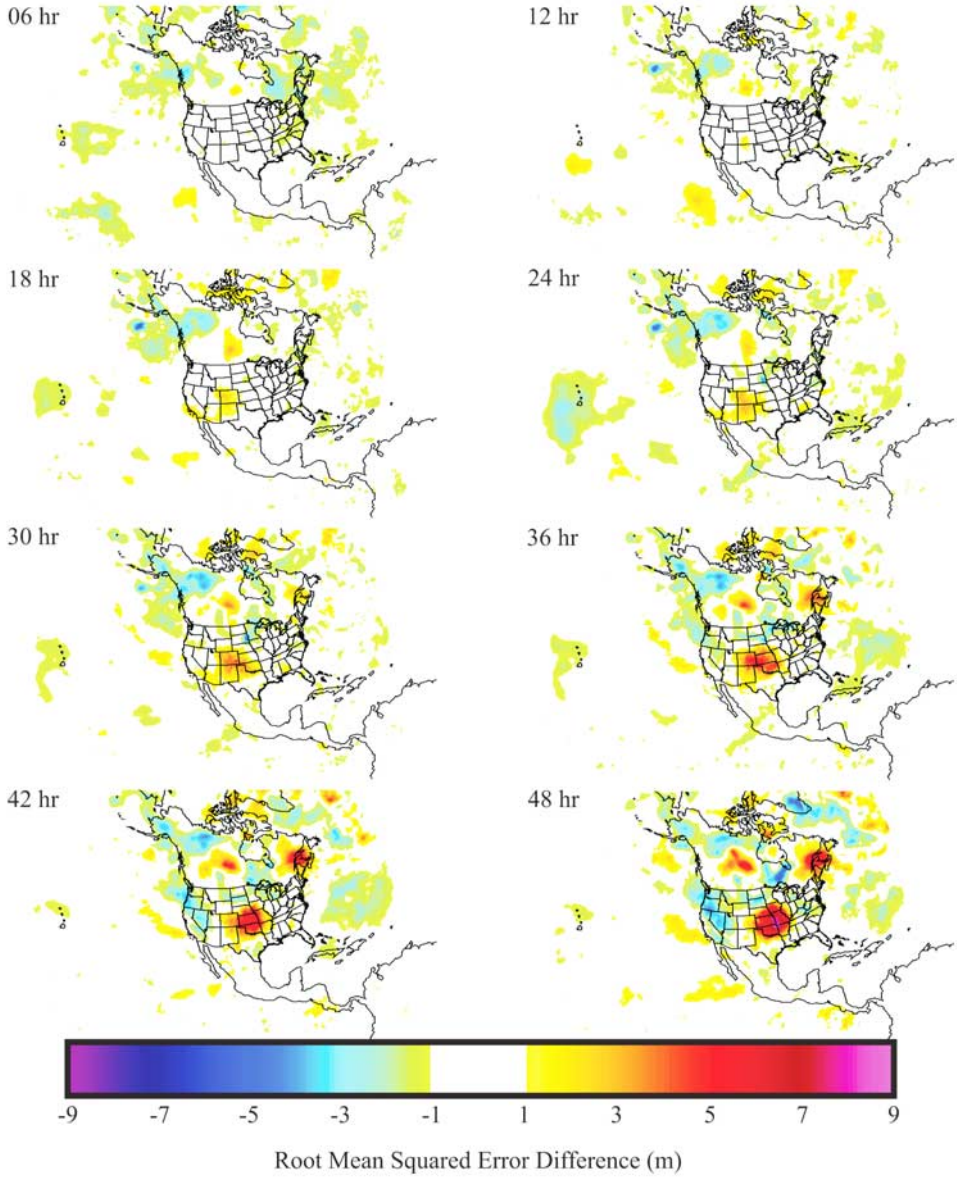

Figure 8. Difference in RMS error between AIRS and CNTL, where warm colors indicate an improvement (reduction) in RMSE with the addition of AIRS measurements and cool colors indicate degradation (increase).

the positive impact region over the central United States, the region exhibited moderate cloud coverage in terms of fraction, roughly 50% (Figure 9) and clouds of varying height (not shown). This region, due to the lowered cloud coverage, had a higher probability of measuring cloud free IFOVs than in the Gulf of Alaska. Also, since the atmosphere had more vertical thermal contrast than the polar regions and clouds were higher vertically, cloud contamination was more easily distinguished in this regime.

[35] Performance measures for forecasted precipitation fields were calculated by comparing the quantitative precipitation forecasts to the Stage 4 precipitation analyses [*Lin and Mitchell*, 2005]. Figure 10 shows the equitable threat scores and bias [*Gandin and Murphy*, 1992] for all 48 h forecasts over the period of study, with scores inclusive of all events greater than the given threshold. Equitable threat scores (ETS) [*Gilbert*, 1884] assess accuracy by considering both correct forecast of nonevents in addition to the correct forecast of events with a score of unity representing a perfect forecast. AIRS precipitation forecast results are neutral, defined as less than ±5% on the CNTL values, at low thresholds, while largest impacts, in terms of percentage improvement or degradation over the CNTL, are seen at 15, 20, and 25 mm $(6\ \mathrm{h})^{-1}$, with improvements of 6%, 6%, and 8%, respectively. The bias scores are defined as the ratio of forecasted points to the number of observed points. A perfect forecast would have a bias score of unity indicating that the forecasted and actual area coverage of precipitation is the same, though a bias score of unity does not necessarily indicate a perfect forecast. Scores less than unity represent an underprediction of precipitation events and those greater than unity represent an overprediction of events. Neutral impact

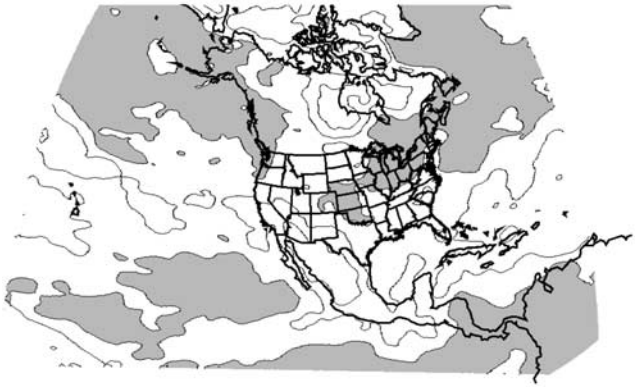

Figure 9. The $1^\circ \times 1^\circ$ 8 day mean cloud fraction, contoured every 25%. Shaded values indicate a cloud fraction greater than 75%.

was generally seen in bias scores with the addition of AIRS measurements to the assimilation system. The largest improvement was seen at the greatest threshold, 25 mm, or roughly one inch, over the six previous hours. In these high impact events, the AIRS data improve precipitation forecasts by 7% over the CNTL.

8. Conclusions

[36] The paper presented an approach for the assimilation of AIRS radiance data into an operational forecast system. The resulting forecasts for the study period indicated that the AIRS had a positive impact on short-term forecasts within a system that emulates the operational NAM system. These improvements stemmed from the improved analysis, as the additional measurements were the only experimental variable. Using appropriate spectral and spatial thinning methodologies, the measurements were shown to adjust the predicted background state toward the observations. This impact was shown to be net-positive, both by the validation of the analysis states and the verification of subsequent forecasts.

[37] It is noted that the period of study for this work is short, thus the statistical sample is small. Ideally, the time period would have been extended beyond 1 week, but computational limitations prevented a longer simulation. Thus the results presented are done so in that they both agree with previous results in the assimilation of AIRS measurements [e.g., *Le Marshall et al.*, 2006; *McNally et al.*, 2006] and present a methodology for the utilization of the measurements within an operational limited-area modeling framework versus a global modeling framework.

[38] The incorporation of the AIRS measurements into the data assimilation system showed, relative to the control, improved agreement to the independent GOES-11 sounder brightness temperature measurements. The largest positive impact was seen in channels with sensitivity to the upper troposphere and lower stratosphere and during times when AIRS observations were assimilated over regions spatially coincident to the GOES sounder measurements (0000 and 1200 UTC). In these cases the inclusion of AIRS data in the system moves the analysis toward the true state, but this improvement is lessened substantially at asynoptic analysis times (0600 and 1800 UTC) when the impact of AIRS data is solely due to analysis increments from previous cycles carried through to the background state. The lack of other independent measurements covering a broader area of the forecast region limits the usefulness of this methodology for initial state validation purposes.

[39] To further test if the atmosphere was in fact better characterized, the NAM was run to investigate the quality of the resulting forecasts. Improvements in the forecasted geopotential height fields demonstrated that the assimilation of AIRS data improved the thermodynamic characterization of the atmosphere. Similarly, improvements of quantified precipitation forecasts, particularly in highest-impact situations, were shown. Negative impacts illustrated regionally tended to be in high latitudes, where infrared remote sensing becomes increasingly complicated due to lower tropospheric heights and temperature inversions. Though the presence of clouds in these regions was investigated, further study must be performed to determine if contamination due to persistent, low clouds in the polar region were in fact the cause of negative impacts in the high-latitude regions.

[40] The small amount of data used in the assimilation process relative to the entire observing system is noted in the background. While the purpose of this paper was to utilize a pseudo-operational system for the assimilation of AIRS measurements, it is worth noting that techniques do exist to further exploit the information content of these measurements. Cloud-affected measurements are currently expunged by the operational GSI analysis system [*Derber and Wu*, 1998; *McNally et al.*, 2000]. *Joiner and Rokke* [2000] suggested that it is possible to extracted additional information content via considering the variational cloud-clearing of contaminated radiances. Recent work has shown that the suggestions of *Joiner and Rokke* [2000] are correct in that cloud-cleared AIRS measurements [e.g., *Susskind et al.*, 2003; *Li et al.*, 2005; *Cho and Staelin*, 2006] can have a positive impact when properly utilized [*Le Marshall et al.*, 2008].

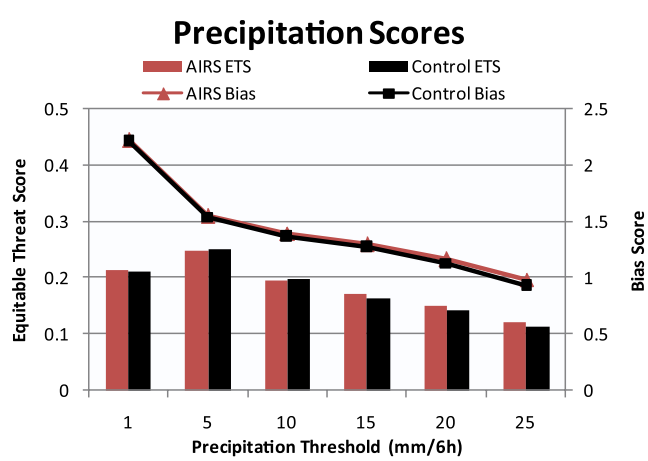

Figure 10. Bias (lines) and equitable threat (bars) precipitation scores for AIRS (red) and CNTL (black). The thresholds indicate the minimum precipitation amount to have fallen over a 6 h period, either in the forecast or analysis, to be considered an event.

[41] The results of this regional assimilation study are promising. The inclusion of additional radiances from the Infrared Atmospheric Sounding Interferometer (IASI) and future instruments such as the Cross-Track Infrared Sounder (CrIS) will allow for greater regional coverage at additional assimilation times and will likely contribute to additional forecast improvement. Similarly, as the operational community moves toward advanced assimilation techniques, the higher temporal resolution of a constellation of hyperspectral infrared sensors or those in from future geostationary platforms would be expected to have a significant impact on forecasts, both in the short and medium range.

[42] **Acknowledgments.** This work was supported by NASA Headquarters under the NASA Earth and Space Science Fellowship Program grant NNG05GQ55H and by Tsengdar Lee of NASA Science Mission Directorate's Earth Science Division in support of the SPoRT program at the NASA Marshall Space Flight Center. The authors would also like to thank Stephen Lord of NCEP, Lars Peter Riishogaard of the JCSDA, and John Le Marshall, formerly of the JCSDA, for providing the computational resources required for this study.

References

Andersson, E., A. Hollingsworth, G. Kelly, P. Lonnberg, J. Pailleux, and Z. Zhang (1991), Global observing system experiments on operational statistical retrievals of satellite sounding data, *Mon. Weather Rev.*, *119*(8), 1851–1865, doi:10.1175/1520-0493(1991)119<1851:GOSEOO>2.0.CO;2.

Aumann, H. H., et al. (2003), AIRS/AMSU/HSB on the Aqua mission: Design, science objectives, data products, and processing systems, *IEEE Trans. Geosci. Remote Sens.*, *41*(2), 253–264, doi:10.1109/TGRS.2002.808356.

Chahine, M. T., et al. (2006), AIRS: Improving weather forecasting and providing new data on greenhouse gases, *Bull. Am. Meteorol. Soc.*, *87*(7), 911–926, doi:10.1175/BAMS-87-7-911.

Chevallier, F., and J.-F. Mahfouf (2001), Evaluation of the Jacobians of infrared radiation models for variational data assimilation, *J. Appl. Meteorol.*, *40*(8), 1445–1461, doi:10.1175/1520-0450(2001)040<1445:EOTJOI>2.0.CO;2.

Cho, C., and D. H. Staelin (2006), Cloud clearing of atmospheric infrared sounder hyperspectral infrared radiances using stochastic methods, *J. Geophys. Res.*, *111*, D09S18, doi:10.1029/2005JD006013.

Derber, J. C., and W.-S. Wu (1998), The use of TOVS cloud-cleared radiances in the NCEP SSI analysis system, *Mon. Weather Rev.*, *126*(8), 2287–2299, doi:10.1175/1520-0493(1998)126<2287:TUOTCC>2.0.CO;2.

Divakarla, M. G., C. D. Barnet, M. D. Goldberg, L. M. McMillin, E. Maddy, W. Wolf, L. Zhou, and X. Liu (2006), Validation of atmospheric infrared sounder temperature and water vapor retrievals with matched radiosonde measurements and forecasts, *J. Geophys. Res.*, *111*, D09S15, doi:10.1029/2005JD006116.

English, S. J., R. J. Renshaw, P. C. Dibben, A. J. Smith, P. J. Rayer, C. Poulsen, F. W. Saunders, and J. R. Eyre (2000), A comparison of the impact of TOVS and ATOVS satellite sounding data on the accuracy of numerical weather forecasts, *Q. J. R. Meteorol. Soc.*, *126*(569), 2911–2931.

Errico, R. M., G. Ohring, J. Derber, and J. Joiner (2000), NOAA-NASA-DoD workshop on satellite data assimilation, *Bull. Am. Meteorol. Soc.*, *81*(10), 2457–2462.

Fourrié, N., and J.-N. Thépaut (2003), Evaluation of the AIRS near-real-time channel selection for application to numerical weather prediction, *Q. J. R. Meteorol. Soc.*, *129*(592), 2425–2439, doi:10.1256/qj.02.210.

Gandin, L. S., and A. H. Murphy (1992), Equitable skill scores for categorical forecasts, *Mon. Weather Rev.*, *120*(2), 361–370, doi:10.1175/1520-0493(1992)120<0361:ESSFCF>2.0.CO;2.

Gilbert, G. K. (1884), Finley's tornado predictions, *Am. Meteorol. J.*, *1*, 166–172.

Goldberg, M. D., Y. Qu, L. M. McMillin, W. Wolf, Z. Lihang, and M. Divakarla (2003), AIRS near-real-time products and algorithms in support of operational numerical weather prediction, *IEEE Trans. Geosci. Remote Sens.*, *41*(2), 379–389, doi:10.1109/TGRS.2002.808307.

Han, Y., P. van Delst, Q. Liu, F. Weng, B. Yan, R. Treadon, and J. Derber (2006), JCSDA Community Radiative Transfer Model (CRTM) version 1, *Tech. Rep. 122*, NOAA, Washington, D. C.

Janjic, Z. I., J. P. Gerrity, and S. Nickovic (2001), An alternative approach to nonhydrostatic modeling, *Mon. Weather Rev.*, *129*(5), 1164–1178, doi:10.1175/1520-0493(2001)129<1164:AAATNM>2.0.CO;2.

Joiner, J., and L. Rokke (2000), Variational cloud-clearing with TOVS data, *Q. J. R. Meteorol. Soc.*, *126*(563), 725–748, doi:10.1002/qj.49712656316.

Le Marshall, J., et al. (2006), Improving global analysis and forecasting with AIRS, *Bull. Am. Meteorol. Soc.*, *87*(7), 891–894, doi:10.1175/BAMS-87-7-891.

Le Marshall, J., J. Jung, M. Goldberg, C. Barnet, W. Wolf, J. Derber, R. Treadon, and S. Lord (2008), Using cloudy AIRS fields of view in numerical weather prediction, *Aust. Meteorol. Mag.*, *57*(3), 249–254.

Li, J., C.-Y. Liu, H.-L. Huang, T. J. Schmit, X. Wu, W. P. Menzel, and J. J. Gurka (2005), Optimal cloud-clearing for AIRS radiances using MODIS, *IEEE Trans. Geosci. Remote Sens.*, *43*(6), 1266–1278, doi:10.1109/TGRS.2005.847795.

Lin, Y., and K. E. Mitchell (2005), The NCEP stage II/IV hourly precipitation analyses: Development and applications, paper presented at the 19th Conference on Hydrology, Am. Meteorol. Soc., San Diego, Calif.

Lorenc, A. C. (1981), A global three-dimensional multivariate statistical interpolation scheme, *Mon. Weather Rev.*, *109*(4), 701–721, doi:10.1175/1520-0493(1981)109<0701:AGTDMS>2.0.CO;2.

McNally, A. P., and P. D. Watts (2003), A cloud detection algorithm for high-spectral-resolution infrared sounders, *Q. J. R. Meteorol. Soc.*, *129*(595), 3411–3423, doi:10.1256/qj.02.208.

McNally, A. P., J. C. Derber, W. Wu, and B. B. Katz (2000), The use of TOVS level-1b radiances in the NCEP SSI analysis system, *Q. J. R. Meteorol. Soc.*, *126*(563), 689–724, doi:10.1002/qj.49712656315.

McNally, A. P., P. D. Watts, J. A. Smith, R. Engelen, G. A. Kelly, J. N. Thépaut, and M. Matricardi (2006), The assimilation of AIRS radiance data at ECMWF, *Q. J. R. Meteorol. Soc.*, *132*(616), 935–957, doi:10.1256/qj.04.171.

Menzel, W. P., and J. F. W. Purdom (1994), Introducing GOES-I: The first of a new generation of geostationary operational environmental satellites, *Bull. Am. Meteorol. Soc.*, *75*(5), 757–781, doi:10.1175/1520-0477(1994)075<0757:IGITFO>2.0.CO;2.

Menzel, W. P., R. A. Frey, H. Zhang, D. P. Wylie, C. C. Moeller, R. E. Holz, B. Maddux, B. A. Baum, K. I. Strabala, and L. E. Gumley (2008), MODIS global cloud-top pressure and amount estimation: Algorithm description and results, *J. Appl. Meteorol. Climatol.*, *47*(4), 1175–1198, doi:10.1175/2007JAMC1705.1.

Michalakes, J., J. Dudhia, D. Gill, T. Henderson, J. Klemp, W. Skamarock, and W. Wang (2004), The Weather Reseach and Forecast model: Software architecture and performance, paper presented at 11th Workshop on the Use of High Performance Computing in Meteorology, Eur. Cent. for Med. Range Weather Forecasts, Reading, U. K., 25–29 Oct.

Pagano, T. S., H. H. Aumann, D. E. Hagan, and K. Overoye (2003), Prelaunch and in-flight radiometric calibration of the Atmospheric Infrared Sounder (AIRS), *IEEE Trans. Geosci. Remote Sens.*, *41*(2), 265–273, doi:10.1109/TGRS.2002.808324.

Parkinson, C. L. (2003), Aqua: An Earth-observing satellite mission to examine water and other climate variables, *IEEE Trans. Geosci. Remote Sens.*, *41*(2), 173–183, doi:10.1109/TGRS.2002.808319.

Pielke, R. A. (1991), Overlooked scientific issues in assessing hypothesized greenhouse gas warming, *Environ. Softw.*, *6*(2), 100–107, doi:10.1016/0266-9838(91)90035-O.

Reale, O., J. Susskind, R. Rosenberg, E. Brin, E. Liu, L. P. Riishojgaard, J. Terry, and J. C. Jusem (2008), Improving forecast skill by assimilation of quality-controlled AIRS temperature retrievals under partially cloudy conditions, *Geophys. Res. Lett.*, *35*, L08809, doi:10.1029/2007GL033002.

Rodgers, C. (1990), Characterization and error analysis of profiles retrieved from remote sounding measurements, *J. Geophys. Res.*, *95*(D5), 5587–5595, doi:10.1029/JD095iD05p05587.

Strow, L. L., S. E. Hannon, S. De Souza-Machado, H. E. Motteler, and D. Tobin (2003), An overview of the AIRS radiative transfer model, *IEEE Trans. Geosci. Remote Sens.*, *41*(2), 303–313, doi:10.1109/TGRS.2002.808244.

Susskind, J., and L. Kouvaris (2006), Contribution of the AIRS shortwave sounding channels to retrieval accuracy, paper presented at Algorithms and Technologies for Multispectral, Hyperspectral, and Ultraspectral Imagery XII, SPIE, Orlando, Fla., 17–21 April.

Susskind, J., C. D. Barnet, and J. M. Blaisdell (2003), Retrieval of atmospheric and surface parameters from AIRS/AMSU/HSB data in the presence of clouds, *IEEE Trans. Geosci. Remote Sens.*, *41*(2), 390–409, doi:10.1109/TGRS.2002.808236.

Tobin, D. C., et al. (2006), Radiometric and spectral validation of Atmospheric Infrared Sounder observations with the aircraft-based Scanning

High-Resolution Interferometer Sounder, *J. Geophys. Res.*, *111*, D09S02, doi:10.1029/2005JD006094.

Wielicki, B. A., and J. A. Coakley (1981), Cloud retrieval using infrared sounder data: Error analysis, *J. Appl. Meteorol.*, *20*(2), 157–169, doi:10.1175/1520-0450(1981)020<0157:CRUISD>2.0.CO;2.

Wu, W.-S. (2005), Background error for NCEP's GSI analysis in regional mode, paper presented at the Fourth WMO International Symposium on Assimilation of Obsevations in Meteorology and Oceanography, Prague, Czech Republic, 18–22 April.

Wu, W.-S., R. J. Purser, and D. F. Parrish (2002), Three-dimensional variational analysis with spatially inhomogeneous covariances, *Mon. Weather Rev.*, *130*(12), 2905–2916, doi:10.1175/1520-0493(2002)130<2905:TDVAWS>2.0.CO;2.

G. Jedlovec and T. L. Miller, Earth Science Office, NASA Marshall Space Flight Center, Huntsville, AL 35812, USA.

W. McCarty, Global Modeling and Assimilation Office, NASA Goddard Space Flight Center, Goddard Earth Sciences and Technology Center, University of Maryland Baltimore County, Mail Code 610.1, 8800 Greenbelt Road, Greenbelt, MD 20771, USA. (will.mccarty@nasa.gov)